ELSEVIER

Journal of Chromatography A, 977 (2002) 173–183

JOURNAL OF CHROMATOGRAPHY A

www.elsevier.com/locate/chroma

Particle size and density distributions of two dense matrices in an expanded bed system

Xiao-Dong Tong, Yan Sun*

Department of Biochemical Engineering, School of Chemical Engineering and Technology, Tianjin University, Tianjin 300072, China

Received 3 April 2002; received in revised form 27 August 2002; accepted 27 August 2002

Abstract

The size and density distributions of two commercial media, that is, Streamline particles and 6% agarose coated steel beads (6AS), in an expanded bed system has been studied with a glass column (26 mm I.D.) modified by side ports. The Streamline particles have a broad size distribution but a relatively uniform density, while the 6AS beads have both broad size and density distributions. The effect of liquid-phase flow velocity, liquid viscosity and settled bed height on the particle size and density distributions is investigated. It is found that the radial mean particle size and density of the two matrices are uniform, while axial classifications are obvious in the expanded beds. For the Streamline, the volume-weighted mean particle size decreases linearly with increasing expanded bed height. For the 6AS beads, however, the mean particle size is even in the axial direction, but the particle density decreases exponentially with the increase of bed height. Moreover, the mean particle size of the Streamline or the density of the 6AS beads is well expressed as a function of the normalized bed height (that is, the ratio of the distance from bed bottom to the expanded bed height). The liquid flow-rate, liquid viscosity and settled bed height influence the mean axial size or density distribution by affecting the expanded bed height.

Keywords: Size distribution; Density distribution; Expanded bed chromatography; Streamline particles; Agarose-coated steel beads

1. Introduction

An expanded bed is a low back-mixing liquid fluidized bed achieved by the purpose-design of the column configuration and solid matrix with a defined size and/or density distribution. The expanded bed technique offers the potential advantages of both packed bed and fluidized bed. The upward flow through the bed of adsorbents provides the higher void fraction within the bed, which makes it possible for the particulate materials to pass through whilst the target bioproduct is adsorbed onto the solid phase. The purpose-design of the column and adsorbents could ensure the ability of the expanded bed, in an identical way to packed bed chromatography, to purify desired products even at higher velocities. Due to its high bed voidage and good column efficiency, expanded bed adsorption (EBA) has been widely employed to directly recover target bioproducts from cell culture broths, cell disruptates and other unclarified feedstocks [1–4].

To achieve tighter control of the separation pro-

*Corresponding author. Tel.: +86-22-2740-2048; fax: +86-22-2740-6590.

E-mail address: ysun@tju.edu.cn (Y. Sun).

0021-9673/02/$ – see front matter
PII: S0021-9673(02)01390-0

cess and obtain greater process efficiency of the expanded bed system, some operation parameters should be investigated further to govern the fluidization process and adsorption performance. In recent years, there has been renewed interest in this subject. The measurement and control of bed height was the scope of the work of Thelen and Ramirez [5], who used the technique based on ultrasonication to monitor the top of expanded bed. Similar work on monitoring expanded bed height has also been presented by Ghose et al. [6]. Bruce et al. [7] performed the effect of column verticality on liquid dispersion and adsorption efficiency in the expanded bed. Chase and co-workers [8,9] compared the performance of different column diameter in terms of the bed expansion, liquid dispersion and breakthrough behaviors.

The distributions of particle size and density within expanded bed system resulted in a distribution of terminal velocities leading to a classification within the expanded bed [10]. The particles with the larger settling velocities were found at the bottom of the bed while those with the smaller settling velocities were at the top end. The lower liquid diffusion level in the expanded bed was obtained because this classification reduced the mobility of the adsorbents. Moreover, the target product diffusion, film mass transport and liquid phase dispersion are also influenced by this classification [11]. However, there has been little work on the quantitative investigation on the particle size and density distributions of the matrices within expanded bed system. Bruce and Chase [12] recommended that the reliable particle size and density distribution of the adsorbents at various heights within the bed could be obtained using the on-line sampling method. Willoughby et al. [13] provided a batch of the size distribution data along the column of Streamline particles (Amersham Pharmacia Biotech, Uppsala, Sweden) at the settled bed height of 0.15 m with twofold bed expansion. Al-Dibouni and Garside [14] divided the fluidized bed column into different parts so as to allow the contents of each section to be analyzed for the axial size distribution. They also provided a classified fluidized bed model to predict the size distribution.

In this work, we measured the particle size and density distributions of two commercially available materials, that is, large-size, mid-density Streamline particles and small-size, high-density 6% agarose coated steel beads (UpFront Chromatography, Copenhagen, Denmark), in a 26 mm I.D. column modified with sampling ports. The liquid dispersion level within the modified column was estimated by the step-input technique with acetone as the tracer, compared with that obtained within a Streamline 25 column (1.0 m×25 mm I.D., Amersham Pharmacia Biotech). The liquid velocity, settled bed height and liquid viscosity were varied to investigate their effects on the axial particle size and density distributions of the two adsorbents in the modified column. As a result, two empirical correlations were formulated to predict the axial size distribution of the Streamline particles and the axial density distribution of the agarose coated steel beads, respectively.

2. Materials and methods

2.1. Materials

Streamline quartz base matrix was provided by Amersham Pharmacia Biotech. The size distribution were scanned with a Mastersizer 2000 unit (Malvern Instruments, Malvern, UK) in the range of 80 to 500 μm (shown below in Fig. 4), with a volume-weighted mean diameter of 210 μm, and the average density measured by a pycnometer (Anhui Fengyang Instruments, Anhui, China) was 1135 kg/m^3 at 20 °C. The 6% agarose coated stainless steel (6AS) beads were obtained from UpFront Chromatography. The bead sizes ranged from 60 to 250 μm (shown below in Fig. 8), with a mean diameter of 127 μm, and a mean density of 2843 kg/m^3. All other chemicals were of analytical grade from local sources.

2.2. The modified column system for sampling

Fig. 1 shows a schematic picture of the modified expanded bed system. A purpose-designed glass column (0.7 m×26 mm I.D.) with a stainless steel mesh (with 74 μm openings) as the liquid distributor and a prolonged top adapter was used for expanded bed experiments. During these experiments, the top adapter in the column was positioned 0.005 m above the bed surface. The glass column was modified with

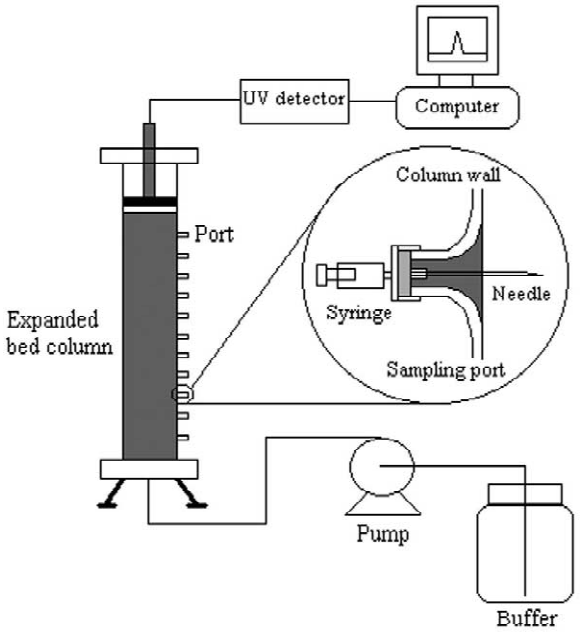

Fig. 1. A schematic diagram of the modified expanded bed system.

10 sampling ports at about 0.05 m intervals up its axial height. Each port was sealed with silicone rubber, and the sealed section is well fit for the smooth inner surface of the column wall. A metal needle (100 mm×1.2 mm O.D.×0.95 mm I.D.) connected to a 2-ml medical syringe was used to withdraw the samples from the column. A peristaltic pump was employed for liquid phase supply. The outlet signal was monitored with a UV detector at 280 nm. The devices were connected using 2.0 mm I.D. plastic tubing. The length of tubing associated with the devices was kept as small as possible to reduce the dead volume in the experimental system. Proper column vertical alignment was confirmed in all experiments.

2.3. Residence time distributions

Liquid dispersion behavior in the expanded bed was determined by residence time distribution (RTD) experiments using the step-input technique. Distilled water and different glycerol solution (20 and 40%, v/v) were used as the liquid phases for expanded bed operations. The expanded beds were performed at 20 °C. In the RTD experiments, 0.25% (v/v) acetone solution was injected as the tracer solution at the bottom inlet of the column, and the output signal at the column outlet was acquired by a personal computer equipped with a data acquisition system. Individual experiments were performed for the complete experimental rig in the presence or absence of adsorbent in order to identify the contribution of the volume of fittings and the 0.005 m zone above the bed surface. The Streamline 25 column connected with ÄKTA explorer 100 (Amersham Pharmacia Biotech) was used as a comparison.

Moment analyses of the RTD data brought out the mean residence time and the variance for the expanded bed system. Considering the expanded bed as a close vessel, the Bodenstein number, Bo, can be calculated from the following formula [15]:

$$\sigma_\theta^2 = \frac{2}{\mathrm{Bo}} - \frac{2}{\mathrm{Bo}^2} \cdot (1 - \mathrm{e}^{-\mathrm{Bo}}) \quad (1)$$

The Bodenstein number relates the ratio of convective to dispersion mass transport, defined as:

$$\mathrm{Bo} = \frac{UH}{\epsilon D_{\mathrm{ax}}} \quad (2)$$

2.4. Sampling and measurements

Typically, the bed was allowed to expand stably for at least 30 min with a corresponding mobile phase. The needle connected with a syringe was inserted into the sealed port, and 1.5 ml of liquid–solid suspension sample was withdrawn from the center or the wall side of the column. To achieve the axial particle size and density distributions within the expanded bed, the sample was withdrawn from the column center up its axial height. As for the radial distributions, the sample was obtained from three radial positions: the column wall apart from sample port, the column center and the column wall near to sample port. The sampling procedure took about 20 s. The mobile phase supplying was then stopped. Then, the particle density of the solid phase in the sample was measured by a pycnometer at 20 °C, and the size distribution was measured with the Mastersizer 2000 unit. The volume-weighted mean particle diameter was used to express the particle size at the sampling position. All the particles were collected to return to the column before the bed was re-expanded

stably for the next sampling. In addition, three repetitive measurements were made for a part of the sampling experiments, and the deviations in the repeated measurements of the particle size and density were found to be less than 5% (data not shown).

3. Results and discussion

3.1. Bed expansion and hydrodynamic characteristics

Hjorth et al. [16] investigated the influence of matrix volume on the turbulence at the column inlet. They demonstrated that the contribution of inlet flow irregularities to the overall mixing could be overcome when the settled bed height was higher than 0.1 m. Therefore, in our experiments, the lowest settled bed height was chosen to be 0.1 m. The results on bed expansion characteristics in the modified column of the two matrices were investigated and compared with those obtained using the Streamline 25 column (standard column) at the settled bed height of 0.1 m. As shown in Fig. 2, the solid phases in the two columns displayed nearly the same bed expansion behavior. Then the effect of the sample ports on liquid dispersion was quantified by RTD analysis. A large discrepancy between the experimental data in the dependence of axial mixing on flow velocity has been reported. For example, Chang and Chase [17] observed that the axial mixing in liquid phase using Streamline SP increased with increasing liquid velocity, while Bascoul et al. [18] described an opposite trend. Dasari et al. [19] reported that the axial mixing increased with increasing liquid velocity for 40- to 63-μm sized LiChroprep Si 60 silica particles but decreased for smaller sized particles (25 to 40 μm). In terms of the literature results, it seems that the axial mixing characteristic depends on the solid phase type, particle size, extent of the particle size and density distributions, the column dimensions and distributor design. In this study, the axial mixing behavior in the standard column of the two matrices as a function of flow velocity was examined and compared with that in the modified column (Fig. 3). As can be seen, increasing liquid velocity led to an increase of Bo from 20 to 42 for the Streamline gels in the standard column. For the 6AS beads, however, the Bo value was fairly constant around 54–62 with the increase of flow velocity. Fig. 3 also shows that the resulting

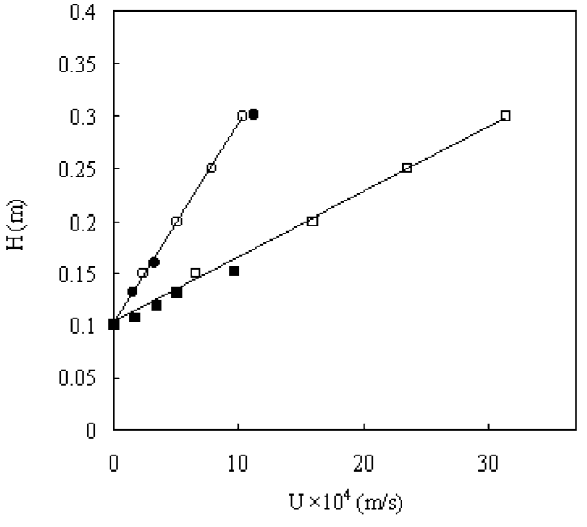

Fig. 2. Bed expansion behaviors in the modified and standard columns with (○, ●) Streamline particles and (□, ■) 6AS beads. The hollow symbols represent the expansion behavior in the modified column, and the solid symbols in the standard column (Streamline 25).

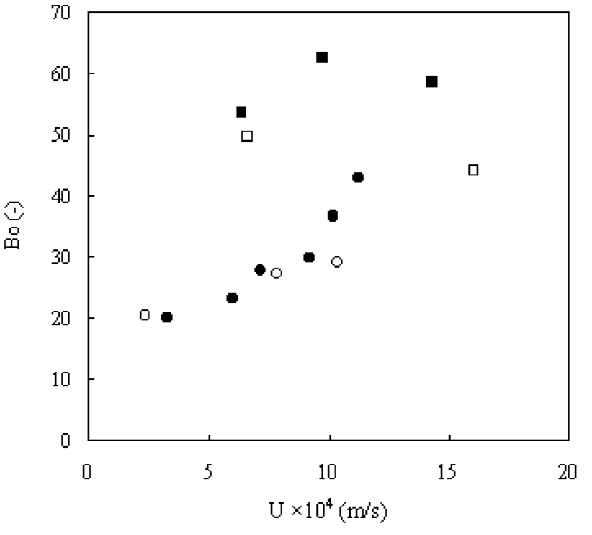

Fig. 3. Axial dispersion behaviors of the two matrices in the modified and standard column (Streamline 25). Symbols and columns are the same as in Fig. 2.

Bo values in the modified column of the two matrices are only slightly lower than those obtained by the standard column at higher liquid velocities. The results indicate that the installation of sample ports gives negligible influences on bed expansion characteristics and liquid dispersion because of the severe sealing by the silicone rubber. In addition, the 6AS beads show higher Bo values than the Streamline gels. A similar observation was reported by Pålsson et al. [20] using the Streamline adsorbents and agarose coated steel beads. They accounted for this observation as the wider density distribution of the agarose coated steel beads, which may result in the more stable bed. The 6AS beads have much wider density distribution, as demonstrated in the following section.

Chang and Chase [17] stated that expanded bed system behaved similarly to a packed bed at Pe >20 (the expression for Pe was the same as Bo as defined by Eq. (2)). As shown in Fig. 3, the Bo values in the modified column are over 20 at the settled bed height of 0.1 m. The increase of Bo with the increase of settled bed height has been well recognized [21,22]. In this work, the settled bed height was higher than 0.1 m, so the Bo values for the modified column experiments were all larger than 20, and the modified expanded bed is considered to simulate well a standard expanded bed system.

3.2. Size distributions of the Streamline particles

Willoughby et al. [13] reported that the radial size distribution of Streamline particles was uniform, and the mean diameter did not change with the distance to center in the column. Similar results were observed in this work (data not shown). In this article, we will mainly describe the axial size distribution of Streamline particles in the expanded bed system.

Examples of particle size distribution at different axial positions are shown in Fig. 4. It can be seen from Fig. 4 that the range of particle sizes at each sampling position is quite large, and the particle size distribution at the lower sampling position is wider than that at the higher position. It is considered due to the liquid and solid-phase mixing within the expanded bed system. Thus, the volume-weighted mean particle diameter (D) was used to express the mean particle size at each sampling position.

The particle size distribution of the sample obtained by us is larger than that reported by Bruce and Chase [12]. This may be due to the difference in the initial particle size (80–500 μm) used in this work and that (Streamline SP of 100–400 μm, 192 μm on average) used by Bruce and Chase [12]. In addition, we consider that the size distribution is sensitive to sample size. The particles up and below the sampling position would be withdrawn during the sampling process, broadening the particle size distribution of the sample in some extent. Thus, to obtain enough particles for measurements and to minimize the effect of sample size on the size distribution broadening, the sample size was set at 1.5 ml of liquid–solid suspension, which was less than 2% of the total bed volume.

From Fig. 4, we can also find that the mean diameter of the Streamline particles decreases with the increase of the sampling height, that is, the distance from the bed bottom (h). To investigate the

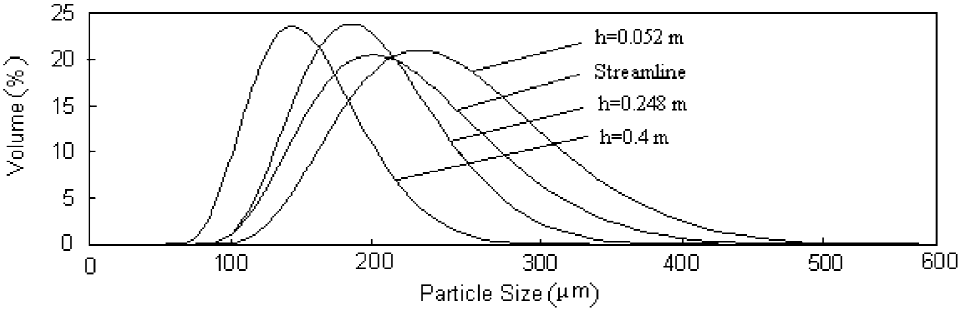

Fig. 4. Examples of size distribution of Streamline particles at the different sampling positions and the batch of Streamline particles. The settled bed height was 0.2 m with a twofold expansion.

changing pattern of the mean particle size with *h*, three major operation parameters, that is, liquid velocity, settled bed height and liquid viscosity, were varied to investigate their effects. The results are exhibited in Fig. 5.

Fig. 5a displays the mean particle size of the Streamline particles as a function of *h* at different liquid velocities. As can be seen, the mean particle diameter decreased approximately linearly with the increase of *h*, and the mean particle diameter increased with the increase of liquid velocity. The effect of settled bed height is similar to that of liquid

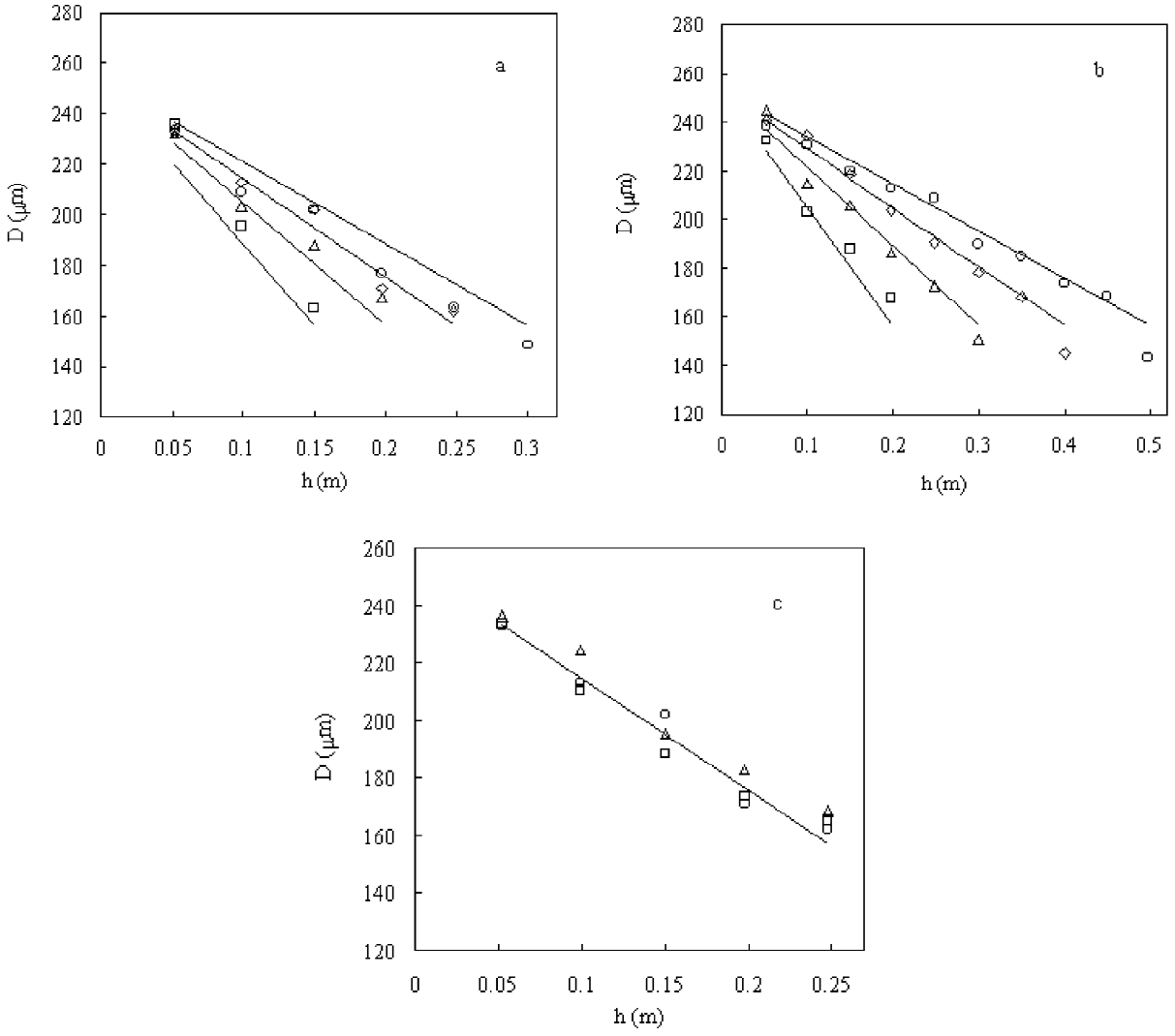

Fig. 5. Volume-weighted mean diameter of Streamline particles as a function of the distance from the bed bottom. (a) Liquid (distilled water) flow velocities were (□) 2.36, (△) 5.0, (◇) 7.78 and (○) $10.28 \cdot 10^{-4}$ m/s, with a settled bed height of 0.1 m. (b) Settled bed heights were (□) 0.1, (△) 0.15, (◇) 0.2 and (○) 0.25 m, each operated at a twofold bed expansion. (c) Liquid phases were (○) distilled water, (□) 20% (v/v) glycerol solution and (△) 40% (v/v) glycerol solution; the settled bed height was 0.1 m with a 2.5-fold bed expansion.

velocity, as shown in Fig. 5b. It indicates that increasing either the liquid velocity or settled bed height leads to the aggravated classification in the column because of the increasing expanded height.

Fig. 5c shows that the variations of liquid viscosity had a negligible effect on the axial particle diameter distribution of the Streamline particles if the expanded bed height is fixed. It should be noted that when the liquid phase was changed from distilled water to 40% glycerol solution, the liquid flow velocity was reduced from 7.78 to $1.98 \cdot 10^{-4}$ m/s to achieve the same expanded bed height. Therefore, the effect of liquid viscosity on the axial particle size distribution of the Streamline particles can be considered to be the effect of liquid velocity. It indicates that the axial size distribution remains unaffected by liquid velocity when the expanded bed height is fixed.

It was difficult to separately analyze the factors influencing the axial size distribution of the Streamline particles because the change of liquid velocity or settled bed height can result in the variation of expanded bed height. Thus, two dimensionless quantities were introduced to discuss these factors: (1) the ratio of the sampling height to expanded bed height (h/H); (2) the ratio of the measured mean diameter at different axial position to the mean diameter of the Streamline particles (D/D_0, $D_0 = 210$ μm). As shown in Fig. 6, a plot of the D/D_0 against h/H under different experimental conditions yields a straight line expressed by Eq. (3):

$$\frac{D}{D_0} = 1.21 - 0.46 \cdot \frac{h}{H} \quad (3)$$

The correlation coefficient (R^2) of Eq. (3) for the experimental data shown in Fig. 6 was estimated at 0.95. The result indicates that the axial mean size distribution of the Streamline particles can be well expressed as a function of h/H. Hence, the liquid flow velocity, liquid viscosity and settled bed height influence the axial size distribution by affecting the expanded bed height (H). In Fig. 6, the experimental data reported by Bruce and Chase [12] is also indicated. As can be seen, Eq. (3) can also well depict their data. This demonstrates that this correlation can be used to describe the axial mean size

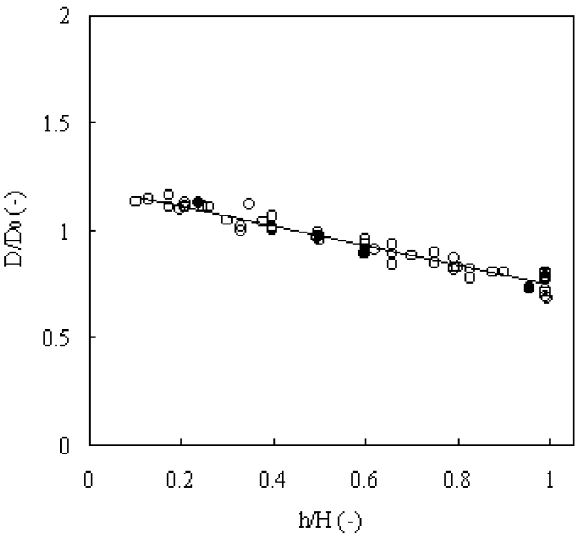

Fig. 6. A correlation between D/D_0 and h/H for Streamline particles. The solid line is calculated from Eq. (3). Solid symbols represent the data from Bruce and Chase [12].

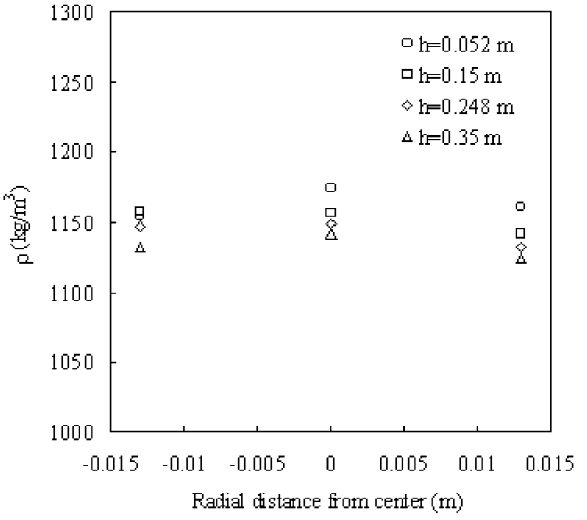

Fig. 7. Examples of axial and radial particle density variations of Streamline particles at four sampling heights. The settled bed height was 0.2 m with a twofold expansion.

distribution of Streamline particles in the expanded bed system.

3.3. Density distributions of the Streamline particles

The particle density of the Streamline particles in the radial direction was measured in different axial positions, and the results are shown in Fig. 7. There was little difference in the mean particle size in the radial direction. Moreover, although the axial mean density slightly decreased with increasing sampling height, the difference was so small that it could be negligible. For example, the mean density was 1131 kg/m^3 at 0.35 m height, and 1174 kg/m^3 at 0.052 m height when the liquid flow velocity was $5.56 \cdot 10^{-4}$ m/s and the settled bed height was 0.2 m. Similar results on the density data are provided in the product catalog of Amersham Pharmacia Biotech [23]. This is due to the relatively uniform density distribution of the Streamline product because it is fabricated by incorporating fine crystalline quartz particles into cross-linked agarose gel.

3.4. Size distributions of 6AS beads

As shown in Fig. 8, the size ranges of the 6AS beads at different sampling heights of expanded bed are nearly the same, and remain unchanged by comparison to the unclassified 6AS beads. Examples of mean size distributions of 6AS beads in the radial and axial directions are shown in Fig. 9. Clearly, there was only a small change in the axial and radial mean particle sizes of the 6AS beads, and this small change was negligible because it was within the experimental error. Therefore, the mean size of the 6AS beads can be considered uniform throughout the whole expanded bed.

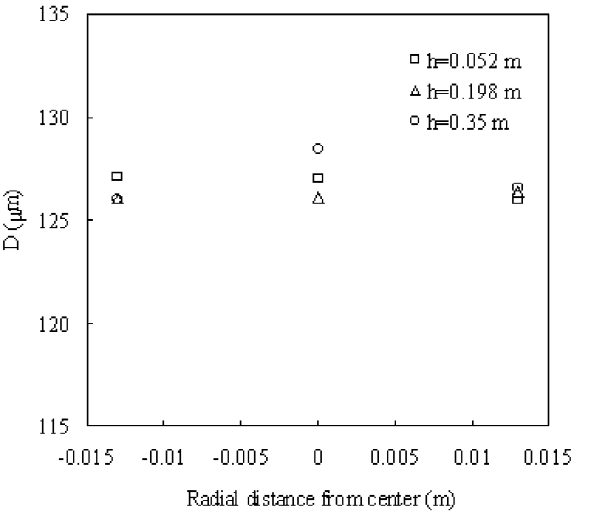

Fig. 9. Examples of radial variations in the mean diameter of 6AS beads at the three sampling heights. The settled bed height is 0.18 m with twofold expansion.

3.5. Density distributions of 6AS beads

The 6AS beads are quite different from the Streamline particles not only in particle size but also in density. As stated in the Materials section, the mean density of the 6AS beads is as high as 2843 kg/m^3. Since the pellicular agarose gel is unevenly coated to steel beads with a mean diameter of 71 μm

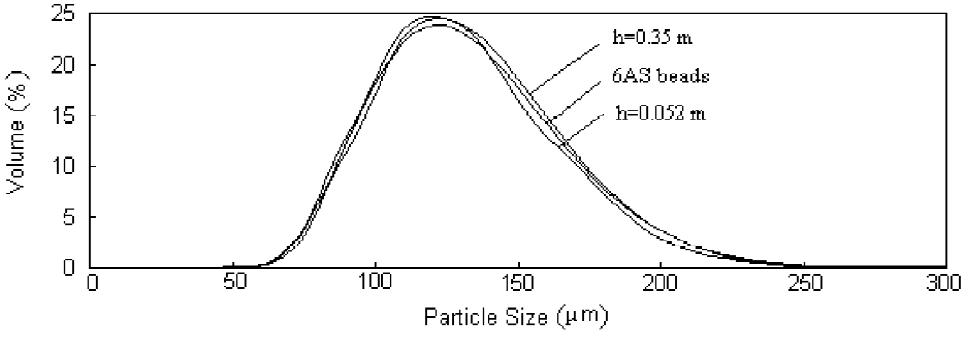

Fig. 8. Examples of size distributions of 6AS beads at different sampling positions and the batch of 6AS beads. The settled bed height was 0.18 m with a twofold expansion.

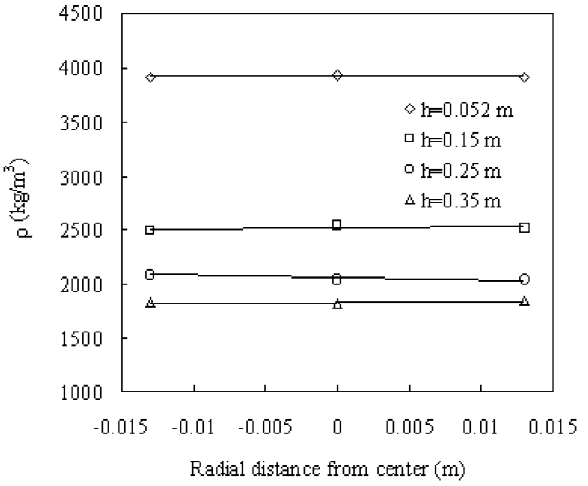

Fig. 10. The radial mean density variations of 6AS beads at the four sampling heights. The settled bed height is 0.18 m with twofold expansion.

[24], the particles are expected to have a wide density distribution.

As shown in Fig. 10, the radial mean density of the 6AS beads is uniform, but the axial density distribution is significant. The mean density decreased from 3927 to 1823 kg/m^3 when the sampling height increased from 0.052 to 0.35 m.

The effects of liquid flow velocity, settled bed height and liquid viscosity on the axial density distribution of the 6AS beads were investigated. Fig. 11 exhibits the results. In all the case studied, the mean density decreased exponentially with increasing h.

Pålsson et al. [20] also prepared agarose coated steel beads, and identified that the composite beads had a wide density distribution. They found that the larger particles had lower density, while the smaller particles had higher density, due to the difference of the agarose volume faction and the amount of the coated steel beads. For the 6AS beads, however, because obvious axial density distribution was found without an axial mean size distribution, it was considered that this solid phase had no obvious statistical (mean) density difference between the larger and smaller particles.

Similar to that for the Streamline particles, the results shown in Fig. 11 can be expressed by a correlation between the ratio of the mean density in the axial direction (ρ) to the mean density of the 6AS beads (ρ_0, 2843 kg/m^3), as shown in Fig. 12. The correlation is as follows:

$$\frac{\rho}{\rho_0} = 0.61 \cdot \left(\frac{h}{H}\right)^{-0.42} \quad (4)$$

The correlation coefficient (R^2) of this equation was estimated at 0.94, indicating that equation are satisfactory for describing the axial mean density of the 6AS beads in the expanded bed system.

4. Conclusions

In this work, we have studied the size and density distributions of the two commercial matrices in the modified expanded bed. The distribution behaviors of the two different matrices were found to be very different from each other. For the Streamline with a relatively uniform density, the larger particles stayed in the bottom of bed while the smaller particles were found in the upper part. For the 6AS beads with a wide density distribution, however, denser particles stayed in the bottom of bed while the lighter particles were found in the upper part, regardless of their particle size. Both the axial distributions of the mean size (Streamline) and the mean density (6AS) were found to be a function of the ratio of the distance from the bed bottom to the expanded bed height. These correlations are expected to be useful in modeling and designing a separation process by expanded bed adsorption. A predictive comparison of these correlations of the particle size and density distributions with a polydisperse hydrodynamic model will be the subject of the next publication.

5. Nomenclature

Bo	Bodenstein number (–)
D	Volume-weighed mean diameter at different axial position (μm)
D_{ax}	Axial mixing coefficient (m^2/s)

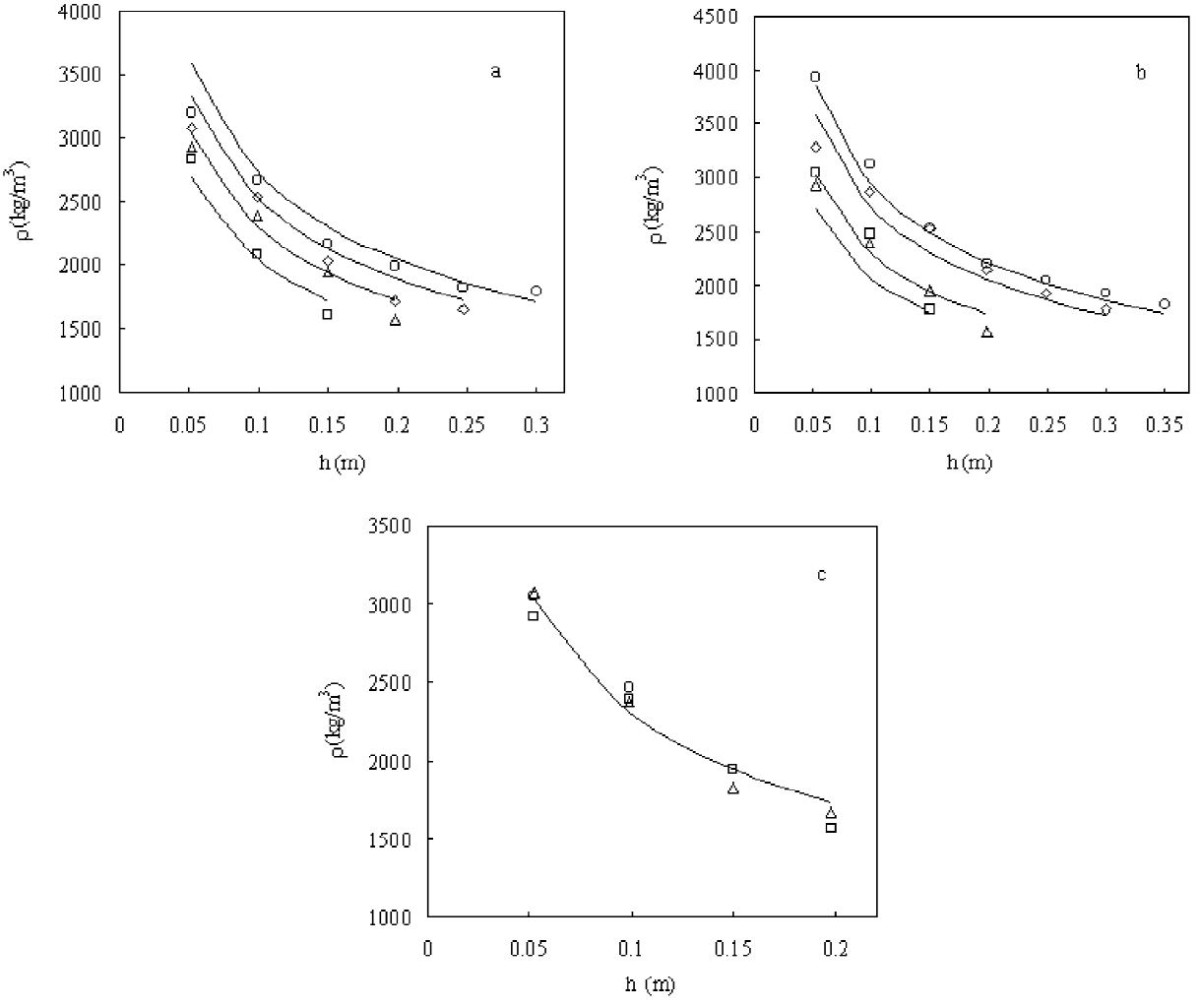

Fig. 11. The factors on the axial density distribution of 6AS beads. (a) The settled bed height is 0.1 m and liquid velocity is (□) 6.67, (△) 16.11, (◇) 23.61, (○) $31.39 \cdot 10^{-4}$ m/s, respectively. (b) The settled bed height is (□) 0.076, (△) 0.1, (◇) 0.15, (○) 0.18 m at twofold expansion, respectively. (c) The liquid viscosity is: (□) distilled water, (○) 20% (v/v) glycerol solution, (△) 40% (v/v) glycerol solution, respectively. The settled bed height is 0.1 m with twofold expansion.

D_0	Mean diameter (μm)
h	Sampling height (m)
H	Expanded bed height (m)
H_0	Settled bed height (m)
U	Liquid superficial velocity (m/s)
Greeks	
ϵ	Voidage of expanded bed (–)
ρ	Mean solid density at different axial position (kg/m^3)
ρ_0	Mean solid density of the whole solid batch (kg/m^3)
σ_θ^2	Variance (–)

Acknowledgements

This work was financially supported by the Natural Science Foundation of China (grant No. 20025617).

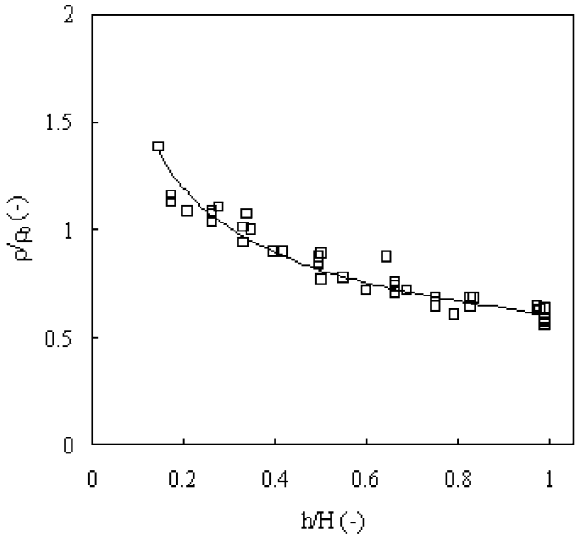

Fig. 12. A correlation between ρ/ρ_0 and h/H for 6AS beads. The solid line is calculated from Eq. (4).

References

[1] R.H. Clemmitt, H.A. Chase, Biotechnol. Bioeng. 67 (2000) 206.
[2] J. Thömmes, M. Halfar, S. Lenz, M.-R. Kula, Biotechnol. Bioeng. 45 (1995) 205.
[3] L.B. Ujam, R.H. Clemmitt, H.A. Chase, Bioprocess Eng. 23 (2000) 245.
[4] G.N.M. Ferreira, J.M.S. Cabral, D.M.F. Prazeres, Bioseparation 9 (2000) 1.
[5] T.V. Thelen, W.F. Ramirez, Chem. Eng. Sci. 52 (1997) 3333.
[6] S. Ghose, H.A. Chase, N. Titchener-Hooker, Bioprocess Eng. 23 (2000) 701.
[7] L.J. Bruce, S. Ghose, H.A. Chase, Bioseparation 8 (1999) 69.
[8] S. Ghose, H.A. Chase, Bioseparation 9 (2000) 21.
[9] S. Ghose, H.A. Chase, Bioseparation 9 (2000) 29.
[10] J. Thömmes, M. Weiher, A. Karau, M.-R. Kula, Biotechnol. Bioeng. 48 (1995) 367.
[11] A. Karau, C. Benken, J. Thömmes, M.-R. Kula, Biotechnol. Bioeng. 55 (1997) 54.
[12] L.J. Bruce, H.A. Chase, Chem. Eng. Sci. 56 (2001) 3149.
[13] N. Willoughby, R. Hjorth, N.J. Titchener-Hooker, Biotechnol. Bioeng. 69 (2000) 648.
[14] M.R. Al-Dibouni, J. Garside, Trans. IChemE. 57 (1979) 94.
[15] O. Levenspiel, Chemical Reaction Engineering, 3rd ed., Wiley, New York, 1999.
[16] R. Hjorth, S. Kampe, M. Carlsson, Bioseparation 5 (1995) 217.
[17] Y.K. Chang, H.A. Chase, Biotechnol. Bioeng. 49 (1996) 512.
[18] A. Bascoul, J.P. Riba, C. Alran, J.P. Couderc, Chem. Eng. J. 38 (1988) 69.
[19] G. Dasari, I. Prince, M.T.W. Hearn, J. Chromatogr. A 631 (1993) 115.
[20] E. Pålsson, P.-E. Gustavsson, P.-O. Larsson, J. Chromatogr. A 878 (2000) 17.
[21] J. Thömmes, M. Weiher, A. Karau, M.-R. Kula, Biotechnol. Bioeng. 48 (1995) 367.
[22] X.-D. Tong, Y. Sun, J. Chromatogr. A 943 (2001) 63.
[23] Amersham Pharmacia Biotech, Expanded Bed Adsorption—Principles and Methods, Handbook, Pharmacia Biotech, Uppsala, 1999.
[24] S. Zhang, Y. Sun, AIChE J. 48 (2002) 178.